# RSC Advances

This is an *Accepted Manuscript*, which has been through the Royal Society of Chemistry peer review process and has been accepted for publication.

Accepted Manuscripts are published online shortly after acceptance, before technical editing, formatting and proof reading. Using this free service, authors can make their results available to the community, in citable form, before we publish the edited article. This *Accepted Manuscript* will be replaced by the edited, formatted and paginated article as soon as this is available.

You can find more information about *Accepted Manuscripts* in the **Information for Authors**.

ROYAL SOCIETY
OF **CHEMISTRY**

www.rsc.org/advances
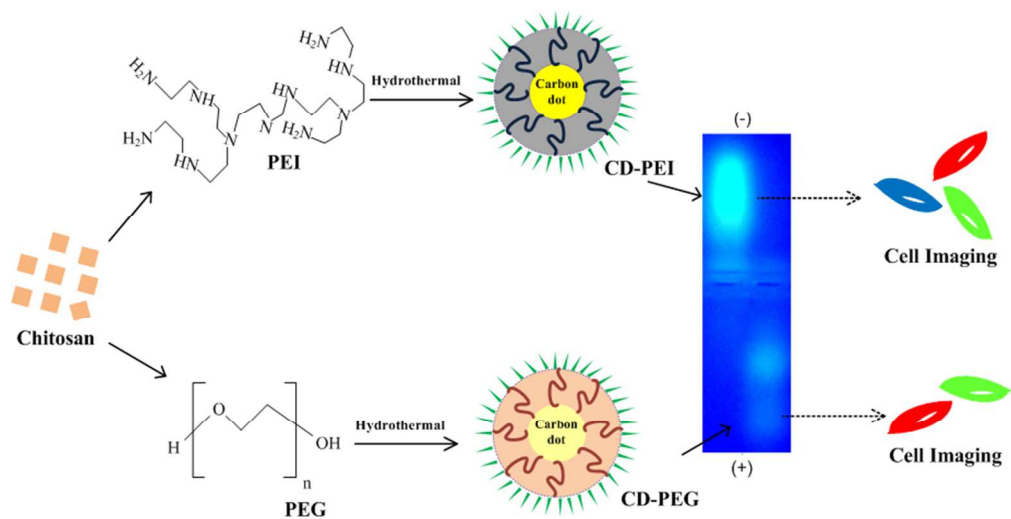
242x124mm (96 x 96 DPI)

ARTICLE TYPE

Implications of surface passivation on physicochemical and bioimaging properties of carbon dots

Abhay Sachdev[a], Ishita Matai[a] and P.Gopinath*[a,b]

The prevalence of surface functionalized carbon dots (CDs) with intriguing fluorescence properties have given a new dimension to the field of bioimaging and perceived as a promising alternative to quantum dots (QDs).In the present work, polyethylene glycol (PEG) and polyethyleneimine (PEI) passivated CDs have been synthesized by one step hydrothermal carbonization of chitosan. We have made a comparative
10 analysis of the physicochemical and bioimaging properties of PEI based carbon dots (CD-PEI) and PEG based carbon dots (CD-PEG). This article further provides an insight into the role of surface functionality in controlling the bioimaging efficiencies of CDs. The concentration dependent cytotoxic effects of CD-PEI and CD-PEG were studied on normal (BHK-21) and cancer (A549) cell lines and explored the competitive performance of CD-PEI compared to CD-PEG for bio-applications.

15 ## Introduction

Luminescent carbon dots (CDs) are a new addition to the world of quantum–sized fluorescent nanomaterials and have shown enormous potential for bio–applications.[1-2] CDs are the most sought-after alternative to toxic heavy metal based semiconductor
20 quantum dots (QDs) for fluorescence related applications, due to their inherent biocompatibility and eco–friendly nature.[1-3]Other remarkable characteristics include broad excitation spectra, multicolor emission, high photostability and colloidal stability. These features endow versatility to CDs and attract their use for a
25 variety of prospective applications, such as sensing, photocatalysis, optoelectronics and energy storage. CDs can be synthesized via top-down approaches, such as arc discharge, electrochemical and laser ablation by breakdown of chunks of carbon structure, which are quite complicated processes and
30 require energy–consuming devices.[1] On the other hand, by using bottom–up approaches like microwave [4-7], solvothermal [8] and hydrothermal treatment [9-12], CDs can be synthesized inexpensively from molecular precursors by means of chemical reactions. Microwave mediated synthesis is a fast and facile
35 route, but the technique is associated with some disadvantages, such as low quantum yield and low brightness of CDs.[5] To alleviate these problems, surface passivation in conjugation with hydrothermal synthesis route can be adopted.[4-6] By this method brighter CDs can be produced in a single step with higher
40 quantum yields and without any post–synthetic treatments. Several passivating agents have been employed for surface modification of CDs, such as polyethylene glycol (PEG) [5,13-14], polyethyleneimine (PEI) [6,15-16], poly(ethylenimide)-co-poly(ethylene glycol)-co-poly(ethyl-enimide) (PPEI) [13,17], 4,7,10-
45 trioxa-1,13-tridecanediamine (TTDDA) [4,12]. The attachment of nitrogen containing moieties onto the surface of CDs has been found to generate stronger fluorescence emission in CDs.

Nevertheless, PEI, an amino rich polyelectrolyte has been used as a passivating agent for CDs more frequently. Chitosan-PEG
50 combination is one such attractive approach for preparation of passivated CDs.[5,18-19]

Bioimaging applications of functionalized CDs have become one of the hot topics of research ever since its inception [3-4,9,12-
55 13,17]. CDs have been delineated for fluorescence imaging of cells due to their excitation dependent behavior, resistance to photobleaching, non–blinking, longer fluorescence lifetimes (nanoseconds) and stability under various cell culturing conditions that satisfies the bioimaging constraints. Sun *et al.*
60 reported the plausibility of PEG and PPEI-EI passivated CDs as bioimaging agents for the first time.[13,17] Thereafter, similar approach was followed in several studies, for example, PEI-modified CDs were found to be non–toxic up to concentrations required for cell imaging and related applications. [6,15-16,20]
65 Conversely, the effect of positive and negative charged surface passivation agents on bioimaging efficiencies of CDs have not been addressed as yet. Mostly CDs emit either in green or blue spectral region, where autofluorescence is significant, which limits its scope for bioimaging. Multicolor CDs that can be
70 excited even at longer wavelengths for red fluorescence emission could be considered as apposite candidates for bioimaging.[4-5,21]

In recent past, the simplicity and generality of preparative protocols for CDs synthesis has been well-documented. CDs can
75 be made from organic matter [5,9,22] and even from natural products, such as soya bean [21], orange juice [23], protein (bovine serum albumin) [10]. Generally, the synthetic strategies of CDs from biological materials is accomplished by pyrolysis of a single precursor that acts as both carbon source and a passivating agent
80 or by employing two components, that is, a passivating agent in

addition to carbon precursor.[1,5,9-10,21] This approach offers a clean, cheap and rapid way of synthesizing CDs in a simplified manner.Herein, we report one-pot hydrothermal synthesis of surface functionalized CDs from chitosan. The surface functionality of the CDs has been tailored by using polymeric passivating agents of different nature (PEI / PEG) under identical reaction conditions. The rationale behind the study is to evaluate the optical performance and bioimaging competence of different surface functionalized CDs. Further, the study investigates their potential as biocompatible imaging agents using BHK-21 (normal) and A549 (cancer) cell lines.

Results and discussion

Hydrothermal based carbonization is a convenient and rapid approach for formation of CD-PEI and CD-PEG. Chitosan has a low carbonization temperature, while PEI and PEG can passivate the surface of CDs due to their respective polyamine and polyhydroxyl structures.[5-6,13-16] Under similar hydrothermal conditions, high temperature and pressure caused the carbonization of chitosan along with simultaneous *in situ* passivation by PEI and PEG to yield CD-PEI and CD-PEG. To eliminate the ambiguity of stability and also to rule out the speculation regarding PEI and PEG being carbonized, both were subjected to hydrothermal treatments under similar conditions in separate experiments. The color of the solutions remained unchanged and no emission was observed. Based on our investigation, we propose the formation scheme for CD- PEI and CD-PEG (Scheme 1).
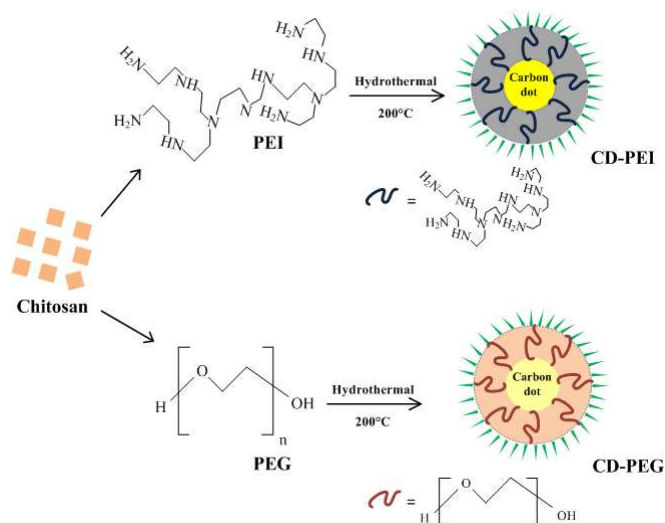
Scheme 1 Schematic diagram depicting one-pot hydrothermal synthesis of CD-PEI and CD-PEG.

The aqueous solutions of CD-PEI and CD-PEG exhibit significant bright green luminescence when irradiated with UV light (inset in Fig. 1(A)).[24] CD-PEI and CD-PEG were also examined for their optical properties. As shown in Fig. 1(A) CD-PEI depicts two absorption bands at 288 nm (π-π^* transition) and 334 nm (n- π^* transition), while CD-PEG shows a single absorption band at 248 nm (π-π^* transition).[5,25] The fluorescence spectra of CD-PEI and CD-PEG depict an excitation dependent

emission phenomenon, as illustrated in Fig. 1(B,C). For CD-PEI, the increase in excitation wavelength from 320 nm to 520 nm resulted in shifting of maximum emission from 445 nm to 554 nm, with a concurrent decrease in emission intensity. The phenomenon of progressive red shift in emission spectra was also observed for CD-PEG, affecting a shift in its maximum emission from 400 nm to 490 nm. It is worth mentioning that shift in emission peak of CDs is an indication of multicolor fluorescence. However, CD-PEI tends to have stronger emission intensity than CD-PEG under similar excitation wavelengths. The maximum emission for CD-PEI and CD-PEG was recorded at an excitation wavelength of 360 nm and 320 nm, respectively. The origin of emission in CDs can be attributed to surface effects contributing to complexity of excited states along with the size dependent effects, as reported previously.[5-6,13,17,25]
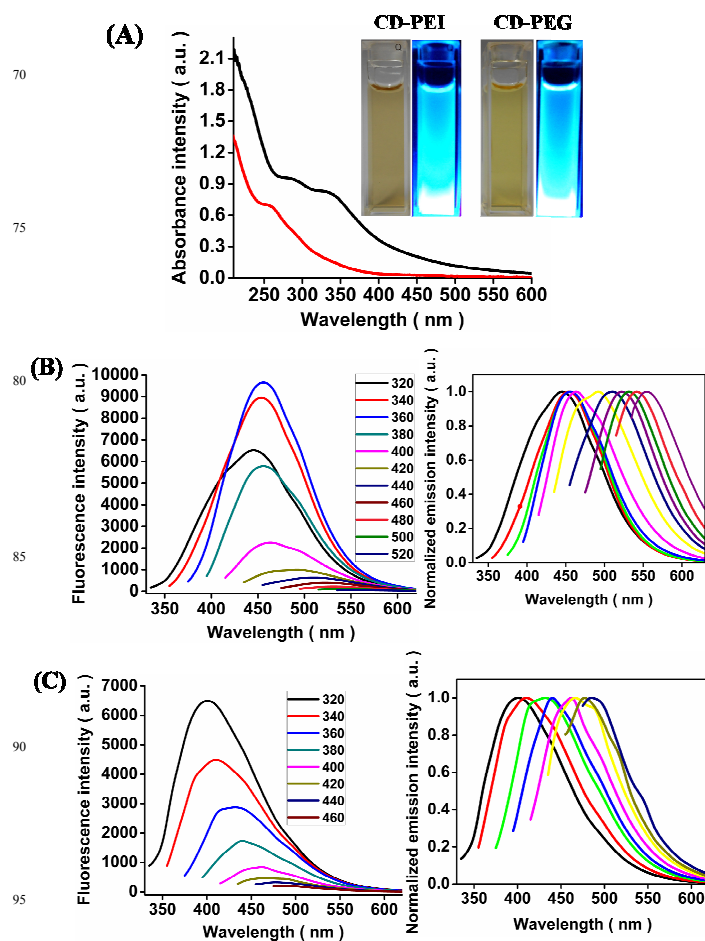
Fig.1 (A) UV-vis absorption spectra of CD-PEI (black) and CD-PEG (red).The insets are the diluted aqueous solution of as-prepared CD-PEI and CD-PEG in ambient light(left) and UV-light (right).(B) Fluorescence emission spectra of CD-PEI at different excitation wavelengths (inset: normalized emission spectra). (C) Fluorescence emission spectra of CD-PEG at different excitation wavelengths (inset: normalized emission spectra).

The quantum yield of CD-PEI and CD-PEG was measured using quinine sulphate as a standard and found to be 13.15% and 7.01%, respectively (Table S1), which was adequately bright for bioimaging as well as higher than our earlier reported values.[5] The fluorescence lifetime decay curve of CD-PEI and CD-PEG

and their average lifetime data have been given in Fig. S1 and Table S2 .For both the samples, the decay curves can be fitted to a triple exponential function, which suggests the presence of multi–radiative species.[11,26] The mean lifetime for CD-PEI and CD-PEG was calculated to be 6.193 ns and 4.825 ns, respectively. Such shorter lifetimes indicate radiative recombination of excitations.[7]

TEM images of CD-PEI (Fig. 2(A)) and CD-PEG (Fig. 2(B)) reveal a pattern of uniform dark dots with near spherical morphology. The average size of CD-PEI and CD-PEG was determined to be 3.4 ± 0.46 nm and 3.9 ± 0.48 nm, respectively from the particle size distributions (insets in Fig. 2). Dynamic light scattering (DLS) measurements predict that CD-PEI and CD-PEG (Fig. S2) have an average diameter around 4.10 nm and 7.85 nm, respectively. In general, the hydrodynamic diameter is slightly larger than dried-state diameter. Similarly, the hydrodynamic diameter in both the cases was bigger than that estimated by TEM, which might be due to polymeric surface passivation of CDs.[27]
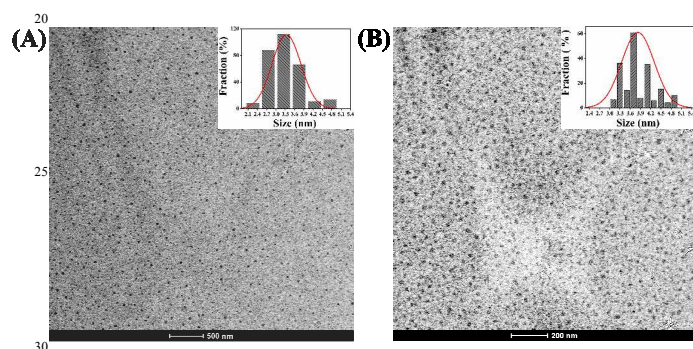

Fig.2 TEM images of CDs.(A) CD-PEI and (B) CD-PEG. The insets are the size distribution histograms of CDs.
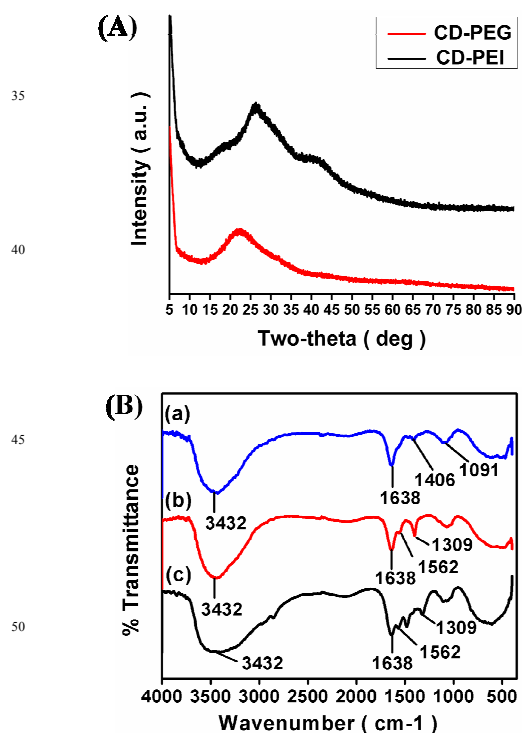

Fig.3 (A) XRD patterns of CDs.(B)FTIR spectrum of (a) CD-PEG,(b) CD-PEI and (c) PEI.

XRD patterns of CD-PEI and CD-PEG (Fig. 3 (A)) display a broad peak at 2θ values of 26.84° and 22.63° respectively, corresponding to (002) plane of nanocarbon. CD-PEI shows an additional weak peak at 2θ = 42.03°, which is attributed to (101) plane. The obtained patterns confirm the amorphous nature of CDs.[15,26,28-29] Fig. S3 represents the EDAX spectrum of CD-PEI and CD-PEG, signifying the presence of carbon, oxygen and nitrogen elements. From the results, it can be seen that the CDs are predominantly composed of carbon. Their composition was mainly dictated by the nature of passivating agent. Higher nitrogen content in CD-PEI probably suggested the presence of amino groups, while higher oxygen content indicated the presence of hydroxyl groups in CD-PEG. The presence of these groups was further explained through FTIR in order to establish the exact chemical nature of CD-PEI and CD-PEG. Notably, the FTIR spectra of CD-PEG shows peaks at 3432 cm^{-1} ,1638 cm^{-1} ,1406 cm^{-1} and 1091 cm^{-1} corresponding to O-H, C=O , C-N and C-O-C groups (Fig. 3(B)) in compliance with our previous study.[5] Furthermore, it is known that chitosan can be carbonized under hydrothermal conditions and pyrolysis results in loss of characteristic vibrations of chitosan saccharide structure.[5,9] As seen in CD-PEI FTIR spectra (Fig. 3(B)), the characteristic absorption peaks of chitosan disappear which indicates carbonization. CD-PEI shares many characteristic peaks of PEI such as N-H at 3432 cm^{-1} and 1562 cm^{-1}, C-N at 1309 cm^{-1} (Fig. 3(B)).[6,15,20] These results reveal that while chitosan got carbonized during pyrolysis, PEI remained stable. Lately, PEI has been reported to be stable up to 200°C, which is in agreement with the obtained results. [15,27] However, a noticeable difference between PEI and CD-PEI lies in the peak at 1638 cm^{-1} (C=O stretching vibration), due to hydrothermal treatment the, C=O peak became sharp and strong for CD-PEI. At the same time, CD-PEI showed less intense N-H peak at 1569 cm^{-1} compared to PEI. These surface functional groups impart hydrophilicity and stability to CDs. No precipitation or aggregation was observed in aqueous solution of CDs for several months.

Agarose gel mobility assay (Fig. 4(A)) was performed to study the surface charge dependent mobility of CDs under electric field. Smear fluorescent bands of CD-PEI and CD-PEG were seen in opposite directions.CD-PEG and DNA migrated towards the positive terminal, while CD-PEI migrated in opposite direction, indicative of the fact that CD-PEI is positively charged and CD-PEG is negatively charged. Sodium dodecyl sulphate-polyacrylamide gel electrophoresis (SDS-PAGE) was done for preliminary investigation of multicolor fluorescence of CDs. CD-PEI shows a single, resolved band (Fig. 4(B)). This underscores the fact that as-prepared CD-PEI was pure. Even more encouraging is the fact that CD-PEI (at such low concentration) was amenable to SDS-PAGE applications.[22] No fluorescent band was observed in case of CD-PEG at concentration equivalent to CD-PEI, owing to its lesser brightness. The excised CD-PEI band depict multicolor fluorescence (Fig. 4(C)), whereas no fluorescence was observed from excised piece of gel (CD-PEG) and blue color was primarily due to background noise.
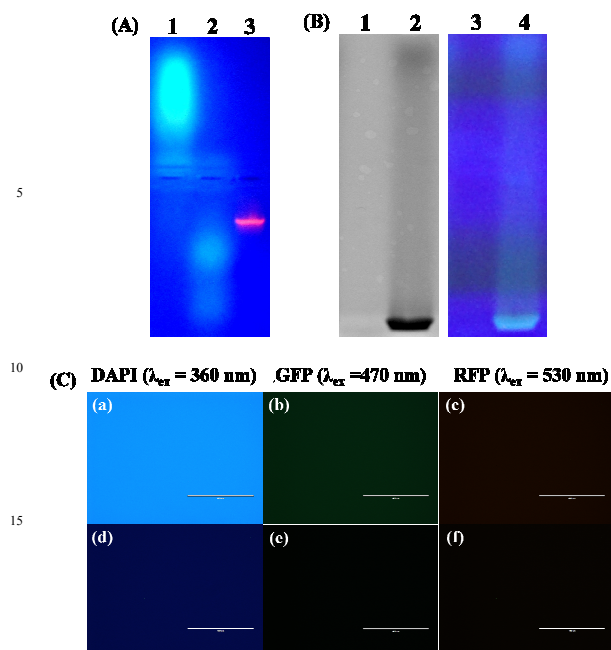
Fig. 4 (A) Agarose gel electrophoretic mobility of CD-PEI (lane 1), CD-PEG (lane 2) and ethidium bromide stained DNA (lane 3) under UV light (λ_{ex} = 365 nm). (B) SDS- PAGE electrophoresis pattern of CD-PEG (lane 1 & 3) and CD-PEI (lane 2 & 4) observed under normal light (left) and UV light (right). (C) Fluorescence microscopic images taken under various excitation filters. Excised gel band of CD-PEI representing multicolor fluorescence (a-c). Excised gel band of CD-PEG (d-f).Scale bar: 400 μm.

pH sensitivity and stability of CD-PEI and CD-PEG

pH sensitive feature of CDs is one of the interesting phenomenon studied over the years.[30] Therefore, fluorescence response of CD-PEI and CD-PEG was investigated at different pH values by adjusting the pH by 0.1N solutions of HCl and NaOH under constant ionic strengths conditions.
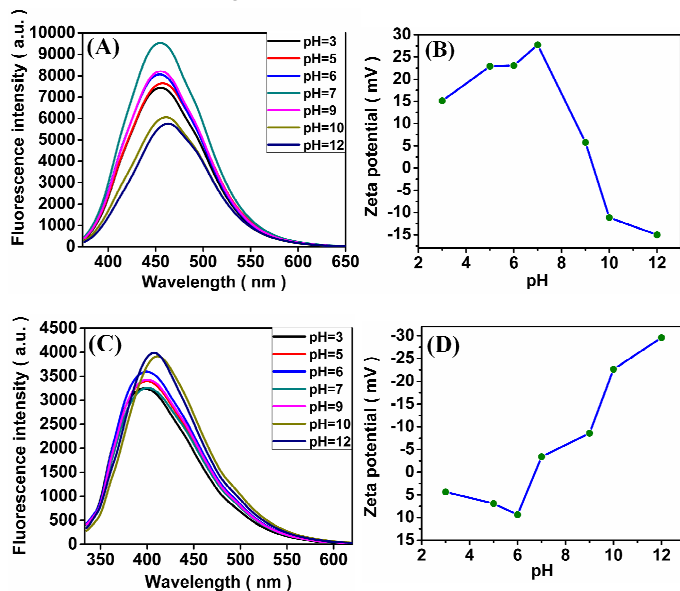
The fluorescence intensity of CD-PEI was found to be pH dependent (Fig. 5(A)). There was a steady increase in fluorescence intensity in the pH range of 3-7, with maximum intensity at pH 7.0. Shift in pH from acidic to basic caused a notable reduction in fluorescence intensity of CD-PEI. The minimum in fluorescence intensity was recorded at pH 12.0. Such pH dependent behavior is due to surface amino groups of PEI, owing to their protonation in acidic condition and deprotonation under alkaline environments.[20] The colloidal stability of CD-PEI over a wide range of pH values was conducted by zeta potential measurements (Fig. 5(B)). The isoelectric point of CD-PEI was found to be pH 9.0.[15] Zeta potential increased dramatically and reached its maximum value (27.7 mV) at pH 7.0, but became very low at pH values above 7.0, with minimum stability at pH 12.0.The excited state pK_a (pK_a*) of CD-PEI was calculated to be 5.04 ± 0.11 based on the change in fluorescence intensity with pH spectra at 460 nm (Fig. S4).[31] Conversely, for CD-PEG, fluorescence intensity was less under acidic conditions (pH 3-6). An apparent increase in fluorescence intensity was evident in the pH range of 7- 12 (Fig. 5(C)).[32] Unlike CD-PEI, a shift in fluorescence emission was observed for CD-PEG from pH 10.0 onwards. The change in surface state brought about by the ionization of surface hydroxyl groups influences the electronic transitions in CD-PEG, giving rise to such pH dependent behavior. Isoelectric point in case of CD-PEG was approximated to be pH 6.0.Contrary to CD-PEI, the zeta potential of CD-PEG was low below pH ≤ 7.0(Fig. 5(D)).There was a marked increase in zeta potential when pH shifted to alkaline. Highly negative zeta potential (-29.6 mV) at pH 12.0 explains the higher stability of CD-PEG under basic conditions. The estimation of highest zeta potential values for CD-PEI and CD-PEG to effect stable particle dispersions are in concurrence with the maximum emission observed at specific pH values.[32]
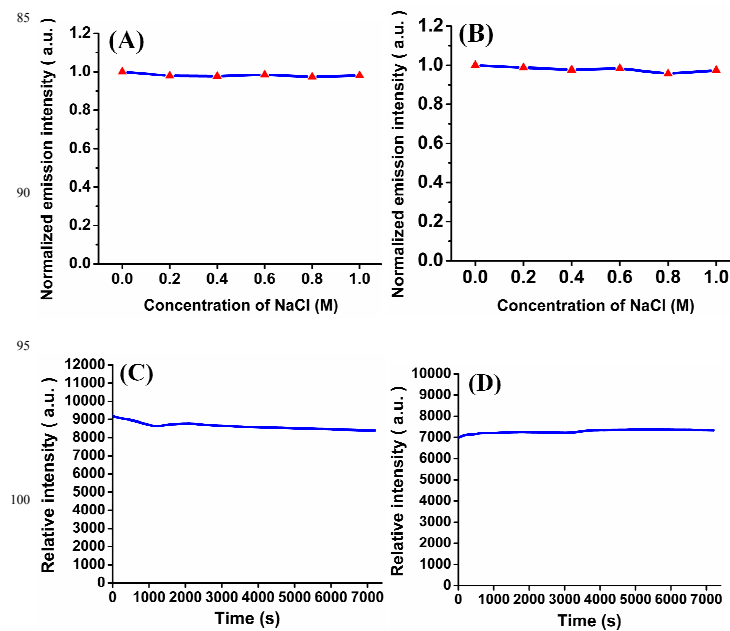

Fig. 5 (A) pH-dependent fluorescence emission spectra of CD-PEI (λ_{ex} = 360 nm).(B) Zeta potential of CD-PEI as a function of pH. (C) pH-dependent fluorescence emission spectra of CD-PEG (λ_{ex} = 320 nm).(D) Zeta potential of CD-PEG as a function of pH.

Fig.6 Plot of normalized emission intensity versus different ionic strength for (A) CD-PEI and (B) CD-PEG. Dependence of fluorescence emission intensity against time showing photostability profile of (C) CD-PEI (λ_{ex} = 360 nm; λ_{em} = 456 nm) and (D) CD-PEG λ_{ex} = 320 nm; λ_{em} = 400 nm).

The effect of varying ionic strengths on the fluorescence intensity of CDs was studied. There were no considerable changes in fluorescence characteristics of CD-PEI (Fig. 6(A)) and CD-PEG (Fig. 6(B)) as NaCl concentration increased from 0.2 to 1.0 M, which is imperative for CDs to withstand high salt concentrations encountered during biological applications.[28]

Moreover, no photobleaching effects were observed for CD-PEI (Fig. 6(C)) and CD-PEG (Fig. 6(D)) under continuous irradiation for 2 h. Fluorescence intensity decreased marginally for both CD-PEI (7.94%) and CD-PEG (4.68%), portraying fairly good photostability. Resistance to photobleaching along with resilience to ionic strength conceive the possibility of using CDs as potential candidates for bioimaging applications compared to organic chromophores.

Bioimaging efficiencies of CD-PEI and CD-PEG

CD-PEI and CD-PEG were evaluated for bioimaging under *in vitro* conditions. We have chosen A549 and BHK-21 cell lines as model systems for bioimaging based on the following considerations. First, A549 cells are lung adenocarcinoma cells which is most prevalent and fatal type of cancer, whereas BHK-21 are normal cells. These provide a platform to examine the bioimaging efficiencies of CDs in both cancer and normal cells. Second, BHK-21 cells differ from A549 cells in terms of morphology; that is, BHK-21 cells are relatively elongated and have a fibroblastic appearance, while A549 cells are epithelial-like cells that possess polygonal morphology. Fig. 7(a-d) shows the fluorescence microscopic images of A549 cells labeled with CD-PEI and CD-PEG. A distinct fluorescence imaging pattern was observed for the two types of CDs. CD-PEI can be clearly seen in the cells depicting blue, green and red color fluorescence, owing to its excitation dependent behavior. However, CD-PEG labeled A549 cells (Fig. 7(e-h)) showed only green and red fluorescent images under similar parameters. BHK-21 cells labeled with CD-PEI (Fig. 7(i-l)) and CD-PEG (Fig. 7(m-p)) demonstrated similar fluorescence profiles. Besides, CD-PEG labeled A549 and BHK-21 cells barely depict any blue color fluorescence under similar microscopic parameters.
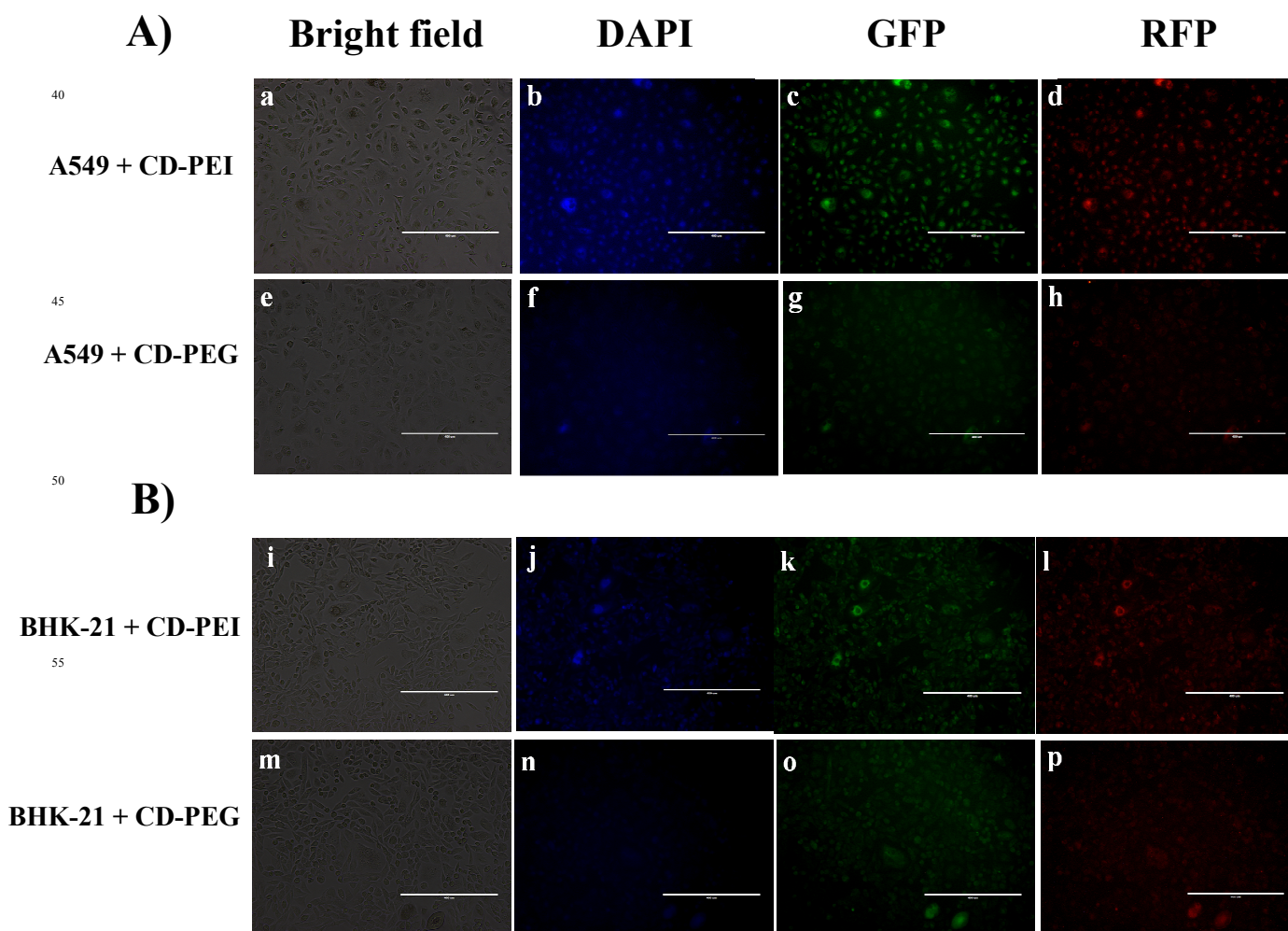
Fig.7 Comparison of fluorescence microscopic images of A549 cells incubated with CD-PEI(a-d) and CD-PEG (e-h).(B) Comparison of fluorescence microscopic images of BHK-21 cells incubated with CD-PEI(i-l) and CD-PEG (m-p). Scale bar: 400 μm. Filters: DAPI (λ_{ex} = 360 nm, λ_{em} = 447 nm)**;** GFP (λ_{ex} = 470 nm; λ_{em} = 525 nm); RFP (λ_{ex} = 530 nm; λ_{em} = 593 nm).

On closer examination two phenomena are evident: (1) labeled A549 cells exhibit bright fluorescence images than labeled BHK-21. This could be due to enhanced cellular uptake of CDs by cancer cells compared to normal cells. (2) Fluorescence microscopic images of CD-PEI and CD-PEG labeled cells testify the excellent bioimaging characteristics of former compared to latter. This outcome seems perfectly rational in terms of physical and chemical properties of CDs. CD-PEI is positively charged due to the presence of amine groups on its surface which was confirmed through zeta potential (fig. 5) and electrophoresis studies (fig. 4(A)). Hence, CD-PEI is more capable of binding to the cell membrane through electrostatic interactions. On the other hand, the overall surface charge of CD-PEG is negative due to presence of PEG chains impeding its interaction with cell membrane. The above investigations clearly acknowledge the fact that the surface functionality to a greater extent influences the bioimaging efficiency of CDs. Meanwhile, one can see ubiquitous distribution of CDs inside the cells. Wide distribution of CDs in the cytoplasm contrary to nucleus (relatively weak fluorescence) was observed due to lesser penetration of CDs, similar to previous published reports.[11-12,17] Quantitative assessment of bioimaging efficiency of CDs were performed by fluorescence spectroscopy and quantum yield measurements. The fluorescence characteristics of CDs labeled A549 cells have been shown in fig. S5. CD-PEI labeled cells had more fluorescence intensity than CD-PEG labeled cells. The obtained fluorescence microscopic images corroborate well with the fluorescence spectroscopic measurements. Additionally, the fluorescence of CDs labeled cells was quantitated through quantum yield measurements. The quantum yield of CD-PEI and CD-PEG labeled cells were 6.55% and 3.49%, respectively.
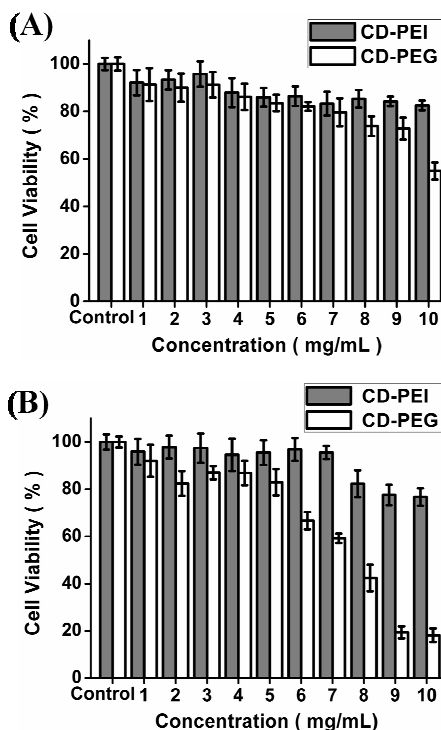
A major concern for bioimaging is the cytotoxicity of fluorescent nanoparticles which limits their applicability. MTT assay was performed in order to determine the optimal concentration of CDs to eliminate the possibility of cell death and detrimental morphological changes during bioimaging.

From the results shown in Fig. 8 (A), it is clear that about 94% of A549 cells were viable up to 3 mg/mL of CD-PEI. When the concentration of CD-PEI was increased to 10 mg/mL, cell viability subsequently declined to 83%. Likewise, A549 cells incubated with CD-PEG showed nearly 90% cell viability up to 3 mg/mL, while severe decline in cell viability was observed beyond 6 mg/mL. MTT plot of BHK- 21 cells (Fig. 8(B)) depict that around 95% cells were viable in the presence of 5 mg/mL of CD-PEI and above 82% of the cells remained viable up to 5 mg/mL concentration of CD-PEG. Previous investigations have shown that CD-PEI is less toxic than PEI for cell based applications due to comparatively lower cationic charge density.[20] Essentially, the maximum concentrations of CD-PEI and CD-PEG estimated through MTT assay were much higher than necessary for bioimaging applications. The results obtained portray biocompatibility and low toxic effects of CDs at concentrations optimal for bioimaging.

Conclusions

In summary, we have devised a facile, eco-friendly and economically viable method for synthesizing intrinsically multicolor, fluorescent PEI and PEG passivated CDs using chitosan as the starting material. The surface passivated CDs demonstrated preeminent properties of tunable emission behaviour, pH sensitivity, small hydrodynamic size, abundant hydrophilic groups, together with resistance to photobleaching and changes in ionic strengths. Even though the carbon source remained the same, fluorescent properties of CD-PEI were amazingly good compared to CD-PEG in terms of strong fluorescence intensity, high quantum yield and longer lifetimes. Interestingly, passivation polymer subjugated the properties of CDs. The proposed study validates the differential labeling capacity of CDs based on surface charge by competitive experiments as well as comparative study on cancer and normal cells. It is worthwhile to mention that the concentration of CDs used for cell imaging did not pose any cytotoxicity. Fluorescence microscopic and spectroscopic analysis predict CD-PEI as a superior bioimaging agent compared to CD-PEG, owing to its efficient fluorescent characteristics and tunable emission from blue to red under cell culture conditions. Designing CDs that are stable in the biological milieu can facilitate the creation of fluorescent nanoprobes for potential biomedical applications. Regarding the surface of CDs, selection of right polymer groups for surface functionalization can enhance its bioimaging efficiency.

Fig.8 MTT based cytotoxicity assay of CDs against (A) A549 cells and (B) BHK-21 cells. The percentage cell viability is assumed to be 100% for control in each case.

Notes and references

ᵃ Nanobiotechnology Laboratory, Centre for Nanotechnology, Indian Institute of Technology Roorkee, Roorkee, Uttarakhand-247667, India. Fax: +91-1332-273560; Tel: 91-1332-285650; E-mail: pgopifnt@iitr.ernet.in, genegopi@gmail.com

ᵇ Department of Biotechnology, Indian Institute of Technology Roorkee, Roorkee, Uttarakhand-247667, India. Fax: +91-1332-273560; Tel: 91-1332-285650; E-mail: pgopifnt@iitr.ernet.in, genegopi@gmail.com

† Electronic Supplementary Information (ESI) available: [details of any supplementary information available should be included here]. See DOI: 10.1039/b000000x/

1. H. Li, Z. Kang, Y. Liu, S-T Lee, *J. Mater. Chem.*, 2012, **22**, 24230-24253.
2. P. G. Luo, S. Sahu, S.-T. Yang, S. K. Sonkar, J. Wang, H. Wang, G. E. LeCroy, L. Cao and Y.-P. Sun, *J. Mater. Chem. B*, 2013, **1**, 2116–2127.
3. L. Cao, S-T Yang, X. Wang, P.G. Luo, J-H. Liu, S.Sahu, Y.Liu and Y-P. Sun, *Theranostics*, 2012, **2**, 295-301.
4. C. J. Liu, P. Zhang, F. Tian, W. C. Li, F. Li and W. G. Liu, *J. Mater. Chem.*, 2011, **21**, 13163–13167.
5. A. Sachdev, I. Matai, S. U. Kumar, B. Bhushan, P. Dubey and P. Gopinath, *RSC Adv.*, 2013, **3**, 16958-16961.
6. C. Liu , P. Zhang , X. Zhai , F. Tian , W. Li , J. Yang , Y. Liu ,H. Wang , W. Wang and W. Liu, *Biomaterials* , 2012,**33**, 3604-3613.
7. H. Zhu, X. L. Wang, Y. L. Li, Z. J. Wang, F. Yang and X. R. Yang, *Chem. Commun.*, 2009, 5118 – 5120.
8. S. Mitra, S. Chandra, S.H. Pathan, N. Sikdar, P. Pramanik and A. Goswami, *RSC Adv.*, 2013, **3**, 3189-3193.
9. Y. H. Yang, J. H. Cui, M. T. Zheng, C. F. Hu, S. Z. Tan, Y. Xiao, Q. Yang and Y. L. Liu, *Chem. Commun.,* 2012, **48**, 380-382.
10. Z .Zhang, J. Hao, J. Zhang, B. Zhang and J. Tang, *RSC Adv.*, 2012, **2**, 8599–8601.
11. Q. Liang, W. Ma, Y. Shi, Z. Li and X. Yang , *Carbon*, 2013, **60**, 421–428.
12. H. Ding, L-W. Cheng, Y.Y. Ma, J-L. Kong, H-M Xiong, *New J.Chem.,* 2013, **37**, 2515-2520.
13. Y- P. Sun, B. Zhou, Y. Lin, W. Wang, K. A. S. Fernando, P. Pathak, M. J. Meziani, B. A. Harruff, X. Wang, H. F. Wang, P. J. G. Luo, H. Yang, M. E. Kose, B. L. Chen, L. M. Veca and S- Y Xie, *J. Am. Chem. Soc.*, 2006, **128**, 7756–7757.
14. Q. Li, T.Y. Ohulchanskyy, R. Liu, K. Koynov, D. Wu, A. Best, R. Kumar, A. Bonoiu and P. N. Prasad, *J. Phys. Chem. C*, 2010**, 114***, 12062–12068.
15. Y. Dong, R. Wang, H. Li, J. Shao, Y. Chi, X. Lin and G. Chen, *Carbon*, 2012, **50**, 2810-2815.
16. J. Kim, J.Park, H. Kim, K. Singha and W.J. Kim, *Biomaterials*, 2013, 34, 7168-7180.
17. L. Cao, X. Wang, M. J. Meziani, F. Lu, H. Wang, P. G. Luo, Y. Lin, B. A. Harruff, L. M. Veca, D. Murray, S.-Y. Xie and Y.-P. Sun, *J. Am. Chem. Soc.*, 2007, **129**, 11318–11319.
18. J. Wu, X. Wang, J.K. Keum, H. Zhou, M. Gelfer, C.A. Avila-Orta, H. Pan, W. Chen, S.M. Chiao, B.S. Hsiao and B. Chu, *J Biomed Mater Res A.,* 2007, **80**, 800-812.
19. L. Casettari, D. Vllasaliu, G. Mantovani, S. M. Howdle, S. Stolnik and L. Illum, *Biomacromolecules*, 2010, **11**, 2854–2865.
20. L Hu, Y Sun, S Li, X Wang, K Hu, L Wang, X Liang and Y. Wu, *Carbon*, 2014, **67**, 508–513.
21. W. Li, Z. Yue, C. Wang, W. Zhang and G. Liu, *RSC Adv.* , 2013, **3**, 20662-20665.
22. H. P. Liu, T. Ye and C. D. Mao, *Angew. Chem., Int. Ed.*, 2007, **46**, 6473-6475.
23. S. Sahu, B. Behera, T. K. Maiti and S. Mohapatra, *Chem. Commun.*, 2012, **48**, 8835-8837.
24. W. Wang, Y. Li, L. Cheng, Z. Cao and W. Liu, *J. Mater. Chem. B* , 2014, **2**, 46-48.
25. B. De and N. Karak, *RSC Adv.*, 2013, **3**, 8286–8290.
26. S.K. Bhunia, A. Saha, A.R. Maity, S.C. Ray and N.R. Jana, *Sci Rep.*, 2013, **3**, 1473-1479.
27. J-Y Yin, H-J Liu, S. Jiang, Y. Chen and Y. Yao, *ACS Macro Lett.*, 2013, **2**, 1033−1037.
28. S. Zhu, Q. Meng, L. Wang, J. Zhang, Y. Song, H. Jin, K. Zhang, H. Sun, H. Wang, and B. Yang, *Angew. Chem. Int. Ed.*, 2013, **52**, 3953 – 3957.
29. S. Pandey, M. Thakur, A. Mewada, D. Anjarlekar, N. Mishra and M. Sharon**,** J . *Mater. Chem. B*, 2013, **1**, 4972-4982.
30. X. Jia, J. Li, E. Wang, *Nanoscale*, 2012, **4**, 5572-5575.
31. J. Zhou, H. Liu, B. Jin, X. Liu, H. Fu and D. Shangguan, *J. Mater. Chem. C*, 2013, **1**, 4427-4436.
32. S. Chandra, P. Patra, S.H. Pathan, S. Roy, S. Mitra, A. Layek, R. Bhar, P. Pramanik and A. Goswami, *J. Mater. Chem. B*, 2013, **1**, 2375–2382.